Atmospheric distortions of spaceborne SAR polarimetric signatures at X and Ka-band

S. Mori[1,2], Frank. S. Marzano[1,2] and N. Pierdicca[1]

1. Sapienza University of Rome, Italy
2. CETEMPS University of L'Aquila, Italy

WHY RAINCLOUDS and SAR ?

- **POTENTIAL of X/Ku/Ka-band SAR for RAIN retrieval**
  - At higher frequency precipitating clouds may produce significant **attenuation/scattering/depolarization** effects
  - The high spatial resolution of SAR sensors might provide new insights into the **structure of precipitating clouds** from space.
  - **Large availability of a new generation of X-SAR satellites** near fully polarimetric

- **Rain effects on SAR imaging and retrieval opportunity**
  - High-resolution microwave rain retrieval from SPACE at a scale below 1 km is only possible from SAR imaging data
  - Rain effect can affect the interpretation of SAR data at X and higher frequencies, **modifying the polarimetric** signature of the ground
  - *Is there a minimum RainSAR retrieval sensitivity at a given spatial resolution (less than 1 km) considering the uncertainty of the surface background?*
  - *Is there an upper limit to RainSAR retrieval? Are there geometrical effects to be solved?*

X-SAR retrievals: Hurricane "GUSTAV" case

South eastern Louisiana around 30.5° N x 89.5° W
September 2, 2008 at 12:00 UTC

TerraSAR-X:
HH pol data

NEXRAD:
S-band
reflectivity
PPI at 0.86 deg
KMOB site

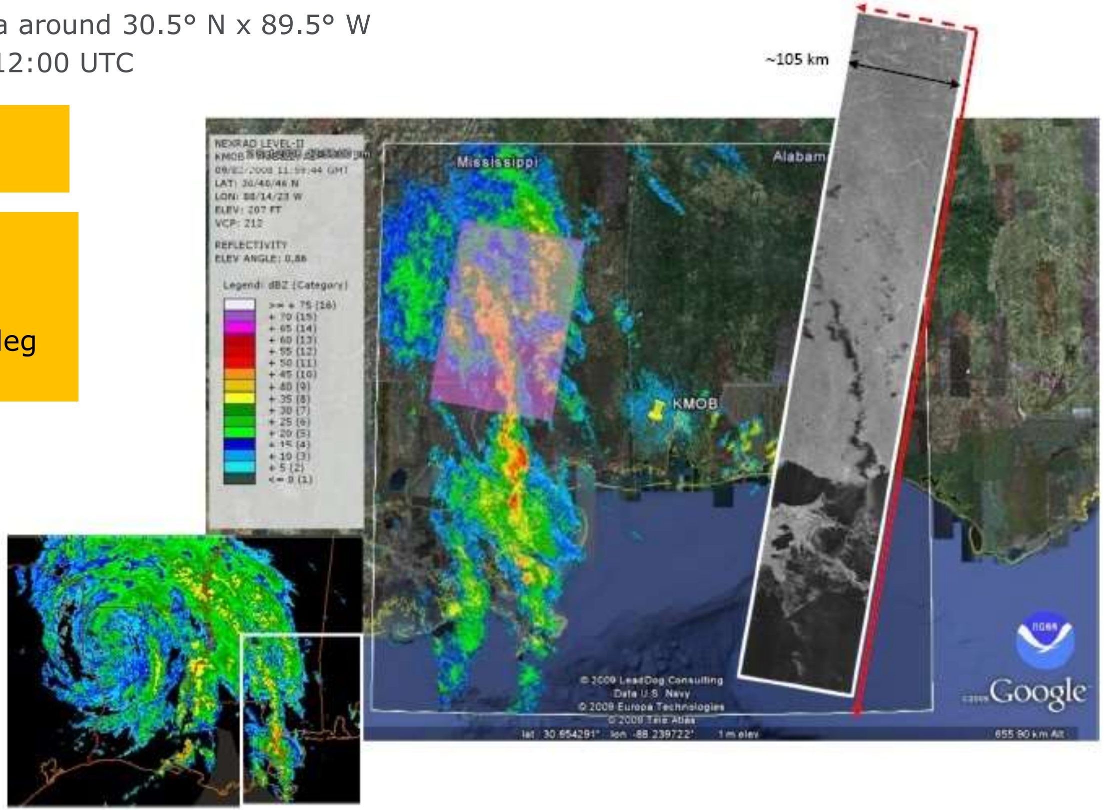

X-SAR retrievals: Hurricane "GUSTAV" case

Precipitation rate [mm/h]

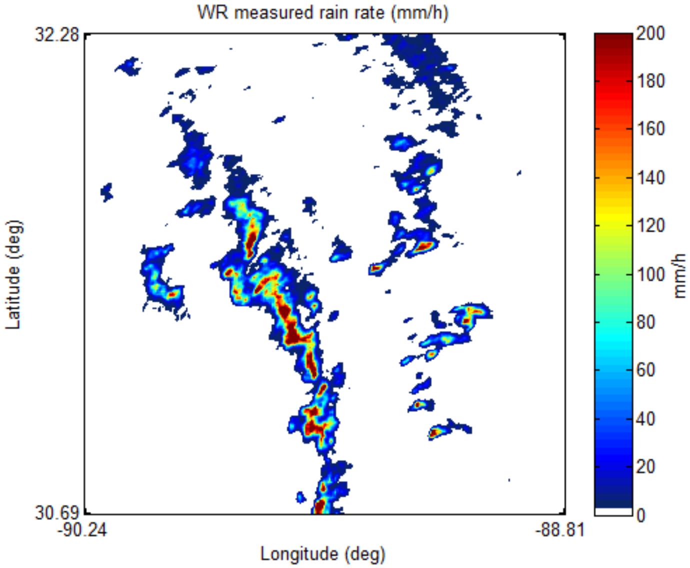

Ground Weather Radar

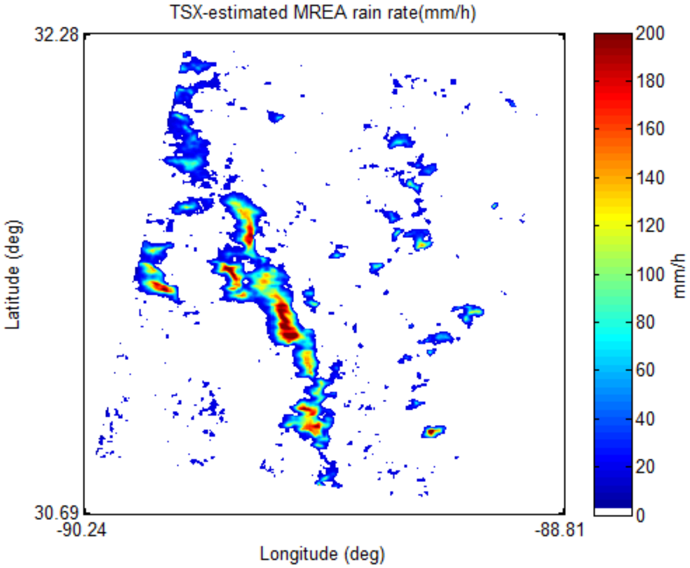

Spaceborne X-SAR

- **Corr = 0.75**
- **Bias = -0.66 mm/h**
- **RMSE = 22.28 mm/h**
- **FRMSE = 0.98**

Outline

Introduction

- Context and examples

Parametric estimation of precipitation from X-SAR

- Case study

Modeling of SAR observations due to precipitation

- SAR response model
- Polarimetric SAR observables
- High-resolution polarimetric simulated scenarios

Polarimetric signature of precipitation

- Sensitivity analysis

Conclusions

SAR cloud response and observables

SAR polarimetric observables

$$\sigma^\circ_{SAR}(x) = \sigma^\circ_{SRF}(x) + \sigma^\circ_{VOL}(x)$$

$$Z_{SARco}(x) = \frac{\sigma^0_{SARhh}(x)}{\sigma^0_{SARvv}(x)}$$

$$\rho_{SARco}(x) = \frac{< S_{SARhh}(x) S_{SARvv}^*(x) >}{\sqrt{< |S_{SARhh}(x)|^2 >}\sqrt{< |S_{SARvv}(x)|^2 >}} = | \rho_{SARco}(x) | e^{j\Psi_{SARco}(x)}$$

- σ^0_{SARpq}: ***pq*-polarized normalized radar cross section (NRCS)**
- Z_{SARco}: **co-polar ratio**
- ρ_{SARco}: **complex correlation coefficient**

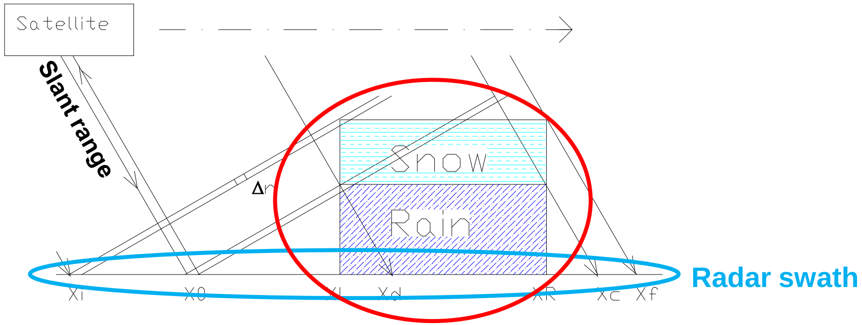

Plane-wave incidence (avoid spherical wave front corrections)

Modelling SAR response: NRCS

- **For a given pixel (*x,y*) the SAR NRCS can be formally expressed as follows:**

$$\sigma^0_{SARpq}(x,y)=\sigma^0_{SRFpq}(x,y)+\sigma^0_{VOLpq}(x,y)$$

  - **$\sigma^0_{SRFpq}(x,y)$:** surface backscatter, attenuated by the two-way path through the precipitating atmosphere
  - **$\sigma^0_{VOLpq}(x,y)$:** volume backscattering due to hydrometeor reflectivity, weighted by the two-way path through precipitating atmosphere

$$\sigma^0_{SRFpq}(x,y)=\sigma^{ground}_{pq}(x,y)\exp\left(-\int_{\Delta l(x,y)}k_{pp}(l)dl-\int_{\Delta l(x,y)}k_{qq}(l)dl\right)$$

$$\sigma^0_{VOLpq}(x,y)=\int_{\Delta t(x,y)}\eta_{pq}(t)\exp\left(-\int_{\Delta l(x,y)}k_{pp}(l)dl-\int_{\Delta l(x,y)}k_{qq}(l)dl\right)dt$$

  - σ^{ground}_{pq}: surface target NRCS
  - η_{pq}, k_{pq}: hydrometeors reflectivity and specific attenuation

$$\eta_{pq}=4\pi<\left|S_{pq}\right|^2>=\int_0^\infty\int_0^{\pi/2}8\pi^2\left|S_{pq}(D,\phi)\right|^2 N(D)p(\phi)dD\sin\phi d\phi$$

$$k_{pq}=-2\lambda<\mathrm{Im}(F_{pq})>$$

  - **S_{pq}, F_{pq}** : element of the complex back or forward hydrometeor scattering matrix
  - **$N(D)$**: particle size distribution
  - **$p(\phi)$**: particle orientation probability density function
  - λ: wavelength

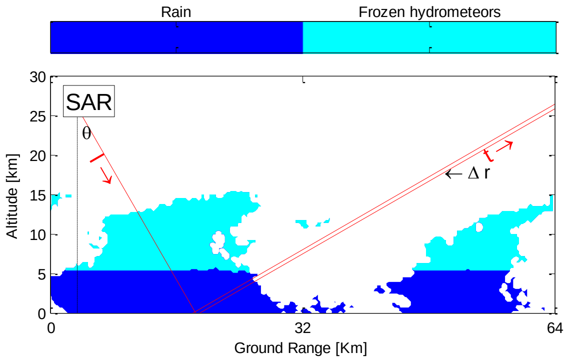

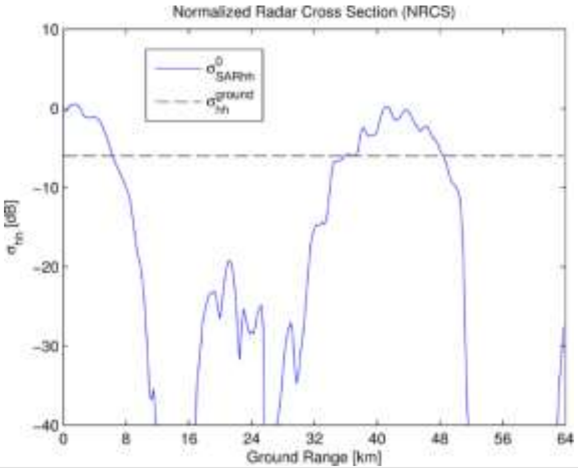

Modelling SAR response: Complex Correlation Coeff.

- **For a ground point (*x,y*) the observable SAR complex correlation coefficient is given by:**

$$\rho_{SARco} = \frac{\sqrt{\sigma^0{}_{hh}}\sqrt{\sigma^0{}_{vv}}\,\rho^{ground}_{co}\, e^{-\int_{\Delta l(x)} k_{hh}(l)dl}\, e^{-\int_{\Delta l(x)} k_{vv}(l)dl}\, e^{j2\Phi co(x)} + sen\theta \int_{\Delta t(x)} C_{VOL}(t)dt}{\sqrt{\sigma^0_{SARhh}}\sqrt{\sigma^0_{SARvv}}}$$

$$\Psi_{SARco}(x,y) = \arg\{\rho_{SARco}(x,y)\}$$

$$C_{VOL}(t) = \sqrt{\eta(t)_{vv}}\sqrt{\eta(t)_{hh}}\,\rho^{vol}_{co}(t)\exp\left(-\int_{\Delta l(t)} k_{vv}(l)dl\right)\exp\left(-\int_{\Delta l(t)} k_{hh}(l)dl\right)e^{j2\Phi_{co}(t)}$$

$$\rho_{co} = |\rho_{co}|\, e^{j\delta_{co}}$$

$$\delta_{co} = \delta_{vv} - \delta_{hh} = \arg(\rho_{co})$$

$$K_{co} = \lambda < \mathrm{Re}(F_{hh} - F_{vv}) >$$

$$\Phi_{co} = \int_{\Delta l(t)} K_{co}(l)dl$$

- ρ_{SARco}, ρ_{co}^{ground}, ρ_{co}^{vol} **:** complex correlation coefficients of observed resolution cell, surface target and volume bin
- δ_{co} : backscatter differential phase
- S_{pq}, F_{pq} : elements of the hydrometeros complex back or forward scattering matrix
- η_{pq}: hydrometeor reflectivity
- K_{co}**:** hydrometeor copolar specific differential phase

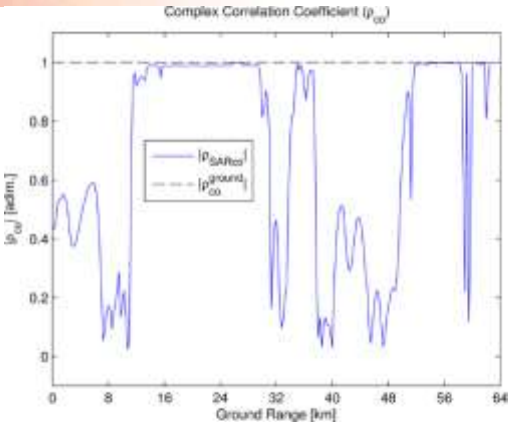

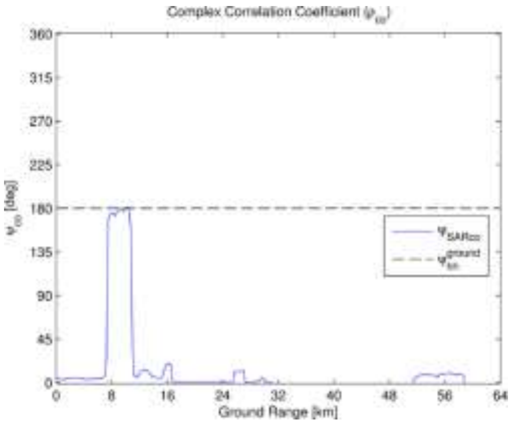

Hydrometeor e.m. parameterization

Hydrometeors polarimetric parameters can be modelled as function of water content by mean of power laws:

$$Z_{epq}(x,y,z) = \frac{\lambda^4}{\pi^5 |K|^2} \eta_{pq}(x,y,z) = a_{Zpq} W(x,y,z)^{b_{Zpq}}$$

$$k_{pq}(x,y,z) = a_{kpq} W(x,y,z)^{b_{kpq}}$$

$$K_{co}(x,y,z) = a_{Kco} W(x,y,z)^{b_{Kco}}$$

$$|\rho_{co}|(x,y,z) = a_{\rho co} W(x,y,z)^{b_{\rho co}}$$

$$\delta_{co}(x,y,z) = a_{\delta co} W(x,y,z)^{b_{\delta co}}$$

- **W** = water content [g/m^3]
- K_{co} = differential phase. [°/km]
- k_{pq} = specific attenuation [dB/km]
- Z_{epq} = equivalent reflectivity [mm^6/m^3]
- $|\rho_{co}|$ = mod. of the copolar corr. Coefficient
- δ_{co} = arg. of the copolar corr. coefficient
- λ = wavelength [cm]
- $|K|^2$ = 0.93 for water and 0.19 for ice

a_{Xpq}, b_{Xpq} coefficients have been obtained by using **APHESS T-Matrix radar scattering model**, as described in [Marzano et al., 2007] and [Marzano et al., 2010].

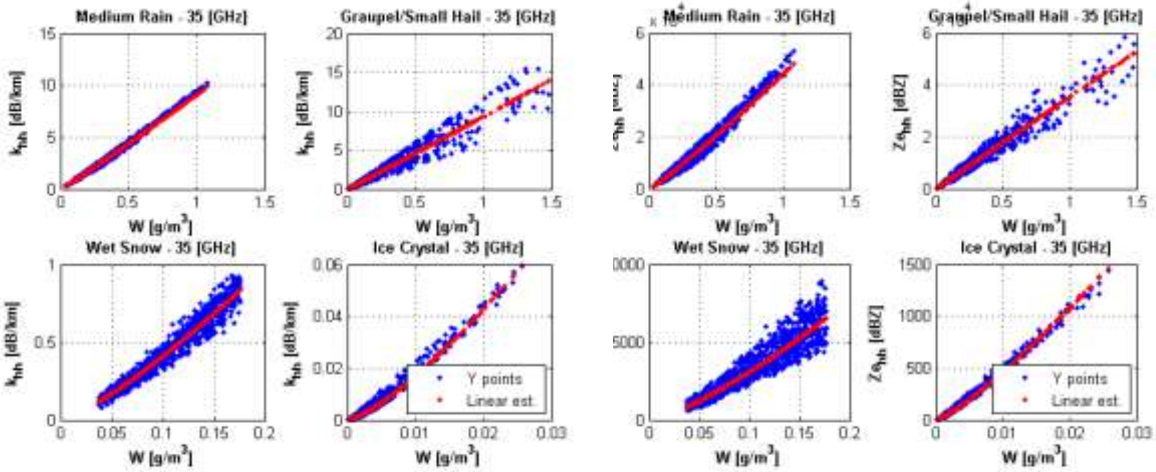

Simulation case studies

The proposed SAR response model requires as input a

- **cloud structure** (2D geometry, hydrometeor types, hydrometeor water content distribution, hydrometeor e.m. response parameterization) and
- the polarimetric characterization of the **ground target**

The ground target polarimetric covariance matrix can be given by:

Models (e.g., bare soil polarimetric response by [Oh et al., 2002]

Polarimetric signature of **canonical targets** (i.e., spheres with ρ_{co}^{ground}=1, dihedrals with ρ_{co}^{ground}=-1, others

The cloud structure (i.e., hydrometeors distributions) can be derived by

ad-hoc **synthetic distributions**, with simplified shape (e.g. parallelepiped), to assess main effects in a simple environment.

Realistic fields simulated by a **3-D high-resolution mesoscale** cloud-resolving models (CRMs)

Simulation of 3D realistic clouds SAR response

The simulated **hydrometeors distributions** can be derived by simulated field through **3-D high-resolution mesoscale cloud-resolving models (CRMs)**

- The **System for Atmospheric Modeling** (SAM) CRM [Blossey et al., 2007] allows at simulating the distribution of Cloud, Rain, Ice, Snow, Graupel particles at 250 m resolution

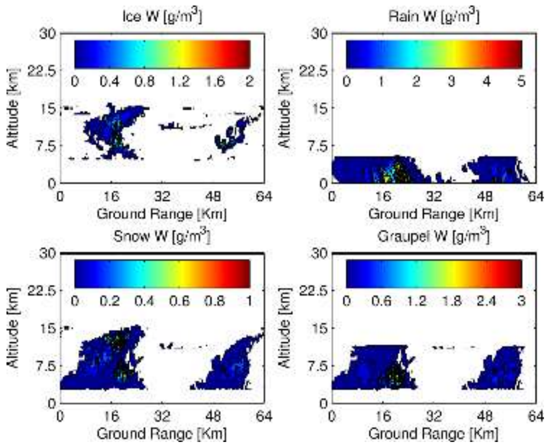

Examples of horizontal and vertical distribution of densities of different hydrometeors predicted by model at a given epoch

- Ground plane σ^0_{SARhh} for **X, Ku and Ka** band, *hh* polarization plus the total **vertically-integrated columnar content** (VIWC).
- The ground response has been considered as constant (about -7 dB at X-band), and so the incident angle (40°).
- The images of the storm are simulated in ground range (the x-y plane), 5 km width, spread all the cross range dimension (64 km).

NRCS [dB]

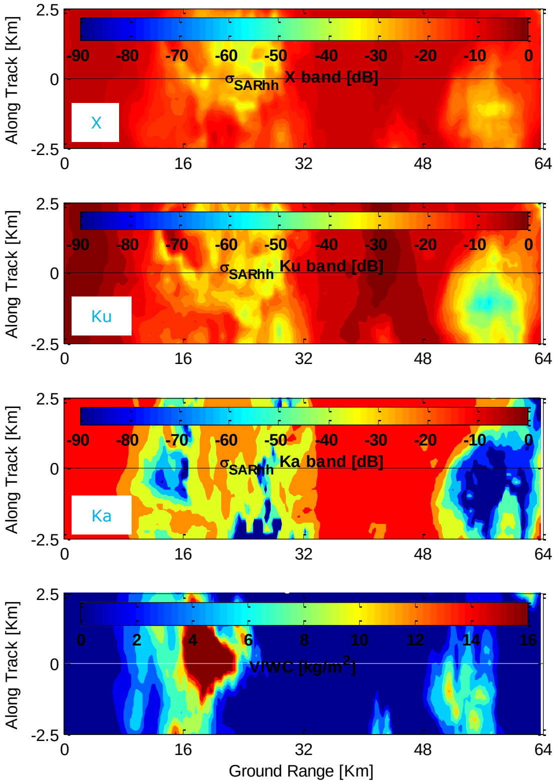

Example: Rectangular cumulonimbus at X-Band

- Parallelepiped structure
- Horizontal uniform 10 km wide hydrometeor density
- **2 vertical layers**: *raindrops 0.3 g/m³* and *snoflakes 0.5 g/m³* water content, with 15 km overall height
- E. M. parameters from revised APHESS T-Matrix model [e.g., Marzano et al., 2007]
- Homogenous background from *bare soil model* [Oh et al., 2002]: *Rms Height* (k_s) *1.5 cm, Correlation Lenght* (k_l) *5.0 cm, Volumetric soil moisture content* (m_v) *0.25* $[cm^3/cm^3]$

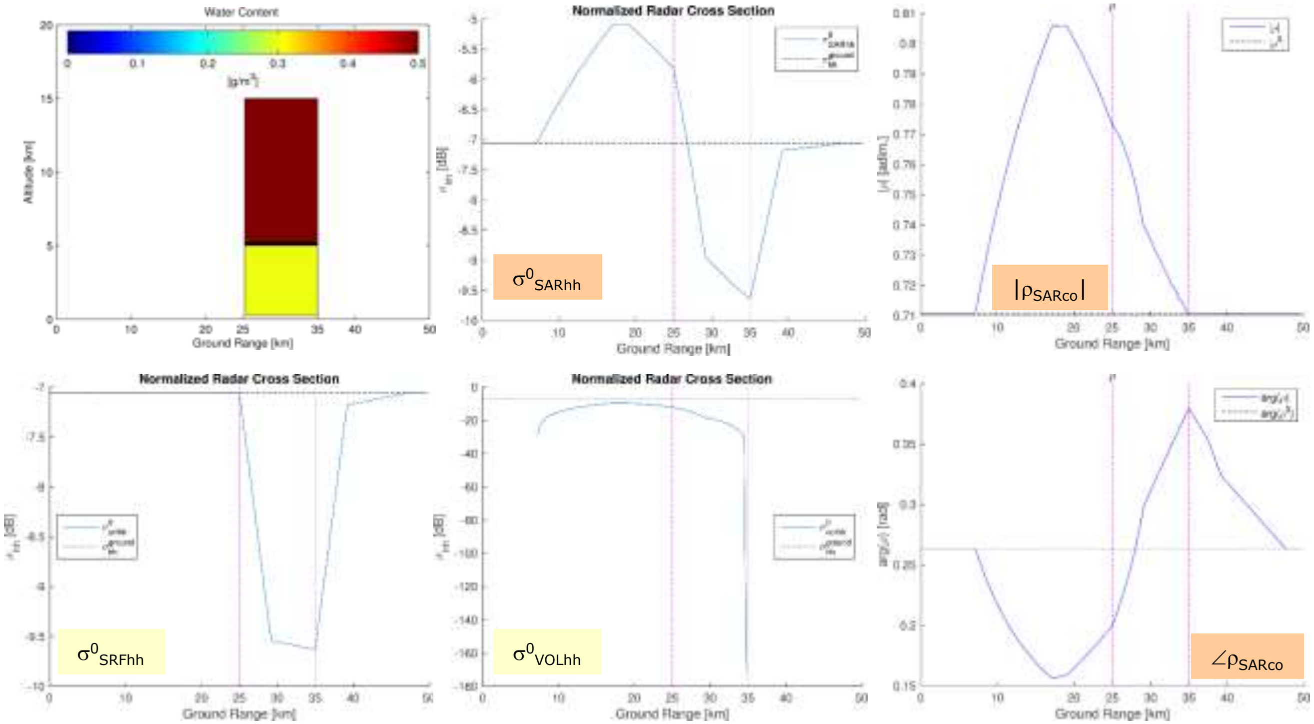

- Zero °C @4.9 km
- $\sigma^{ground} \cong -6$ dB
- f = **9.6 GHz**
- θ=40 deg

Example: Rectangular cumulonimbus at Ka-Band

- Parallelepiped structure
- Horizontal uniform 10 km wide hydrometeor density
- **2 vertical layers**: *raindrops 0.3 g/m³* and *snoflakes 0.5 g/m³* water content, with 15 km overall height
- E. M. parameters from revised APHESS T-Matrix model [e.g., Marzano et al., 2007]
- Homogenous background from *bare soil model* [Oh et al., 2002]: *Rms Height (k_s) 1.5 cm, Correlation Lenght (k_l) 5.0 cm, Volumetric soil moisture content (m_v) 0.25 [cm³ /cm³]*

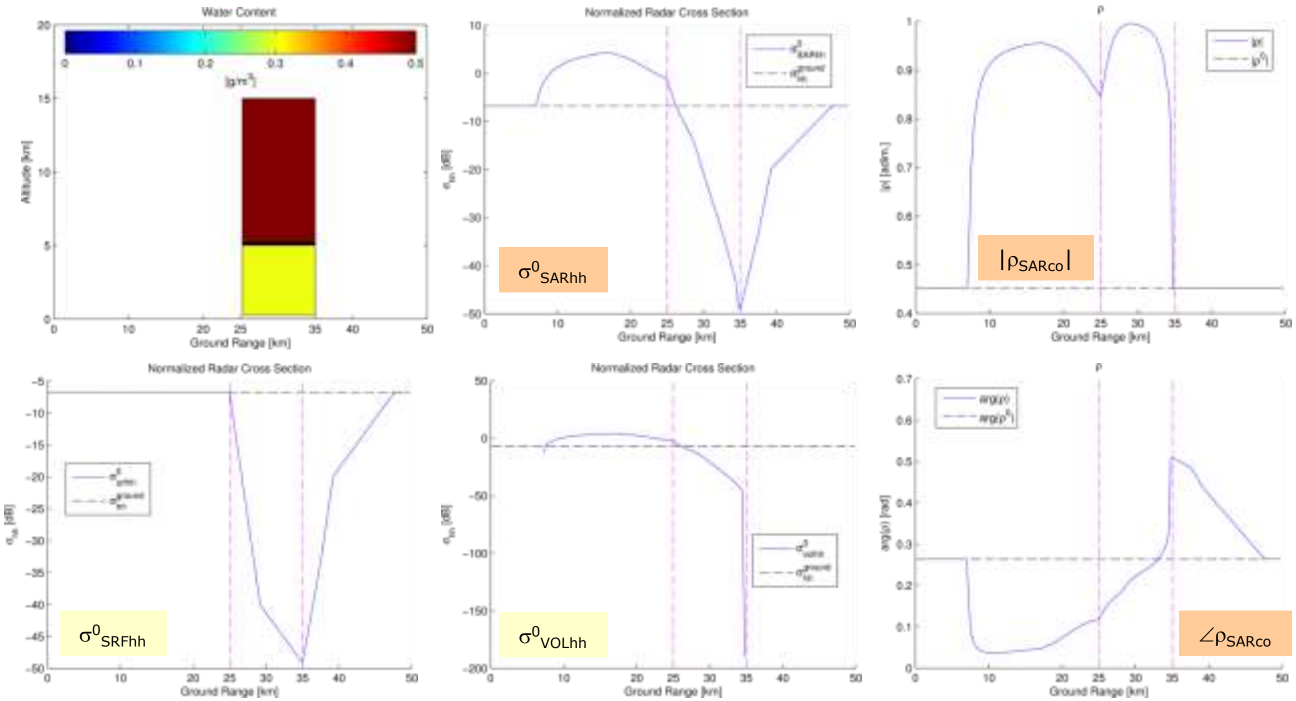

- Zero °C @4.9 km
- $\sigma^{ground} \cong$ -6 dB
- f = **35 GHz**
- θ=40 deg

Outline

Introduction

- Context and examples

Parametric estimation of precipitation from X-SAR

- Case study

Modeling of SAR observations due to precipitation

- SAR response model
- Polarimetric SAR observables
- High-resolution polarimetric simulated scenarios

Polarimetric signature of precipitation

- Sensitivity analysis

Conclusions

Case 1(A): Altostratus (liquid particles sensitivity)

- Non-precipitating cloud
- Ice crystals **0.5 g/m³** 2km height
- Cloud Liquid **{0.001, 0.01, 0.1, 1.0} g/m³** 2km height
- Ground: dihedral corner reflectors 0.025 m

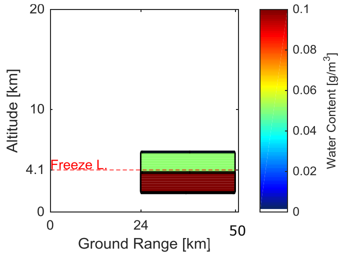

- Detectable only at Ka-band, also 0.001 g/m³ particles
- No phase rotation except Ka-band 1 g/m³
- Polarimetric effects at X-Band, also at 0.001 g/m³

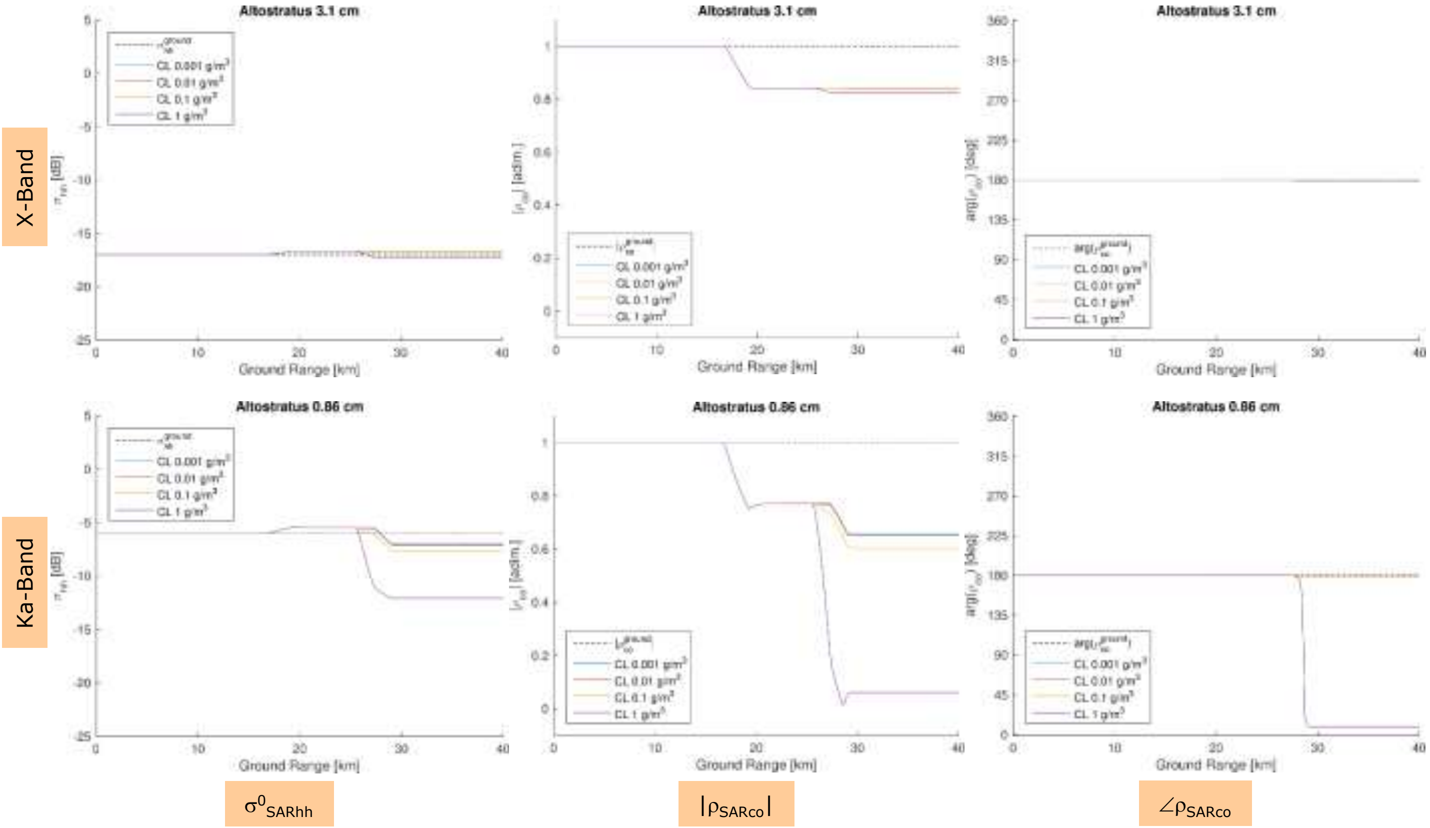

Case 1(B): Altostratus (frozen particles sensitivity)

- Non-precipitating cloud
- Ice crystals **{0.001, 0.01, 0.1, 1.0} g/m³** 2km height
- Cloud Liquid **0.2 g/m³** 2km height
- Ground: dihedral corner reflectors 0.025 m

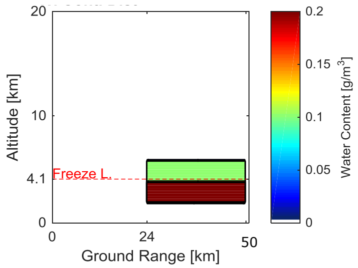

- X-Band sensitive only to high densities of ice
- Ka-band sensitive to ice, especially for W > 0.01 g/m³
- Ka loss of polarimetric coherence for IC ~ CL
- Ka phase rotations for W >= 0.1 g/m³

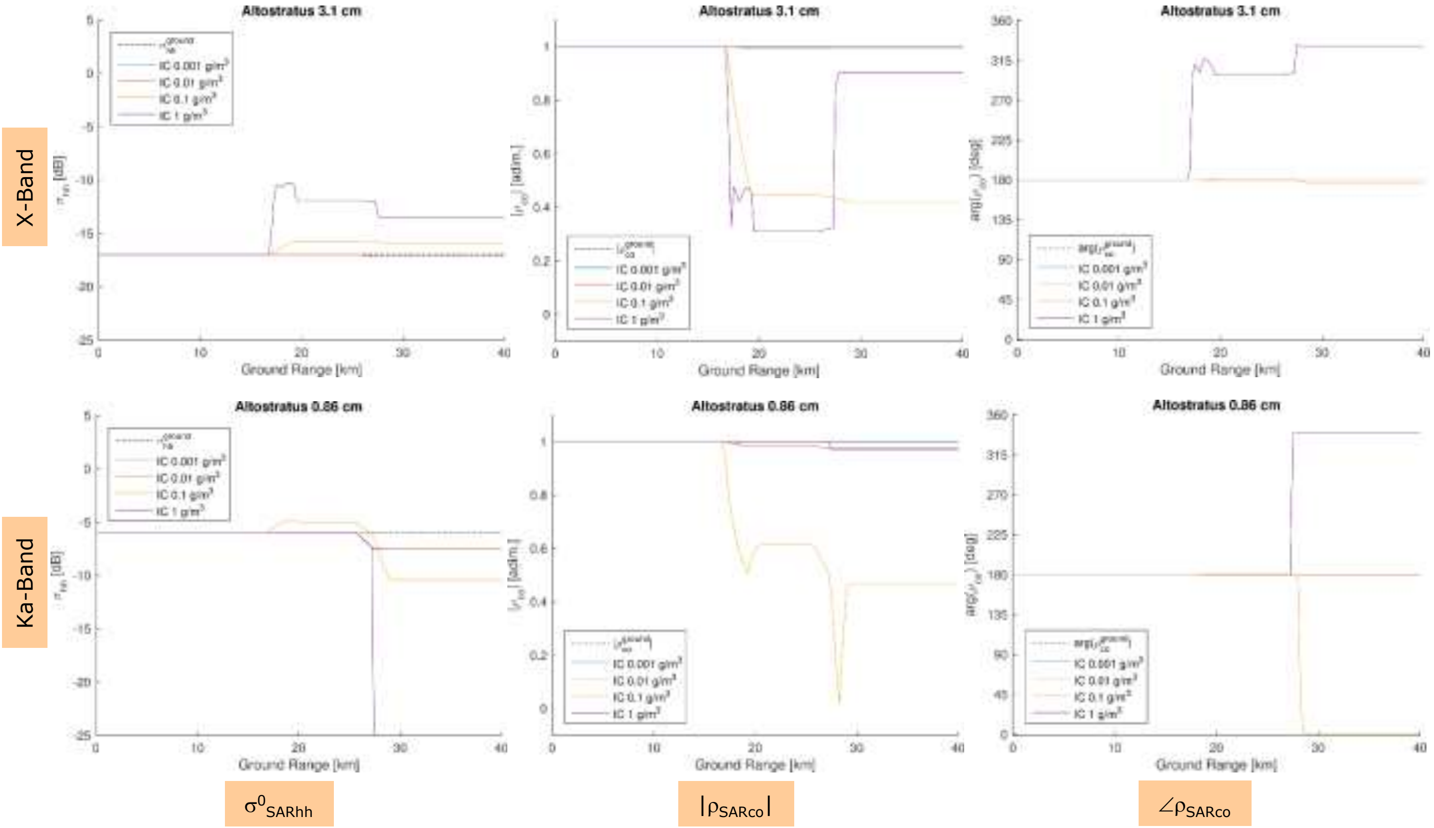

Case 2(A): Nimbostratus (liquid particles sensitivity)

- Precipitating cloud
- Ice crystals **0.5 g/m³** 2km height
- Light Raindrops **{0.001, 0.01, 0.1, 1.0} g/m³** 4km height
- Ground: dihedral corner reflectors 0.025 m

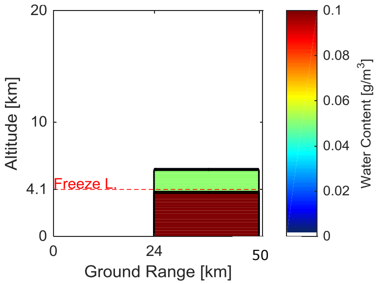

- Precipitation signature at Ka-band, for every densitiy
- At X-Band only 1 g/m³ causes volumetric effects (actually not-detectable NRCS)
- Loss of polarimetric coherence for every band and density
- Phase rotation and increased coherence for highest densities

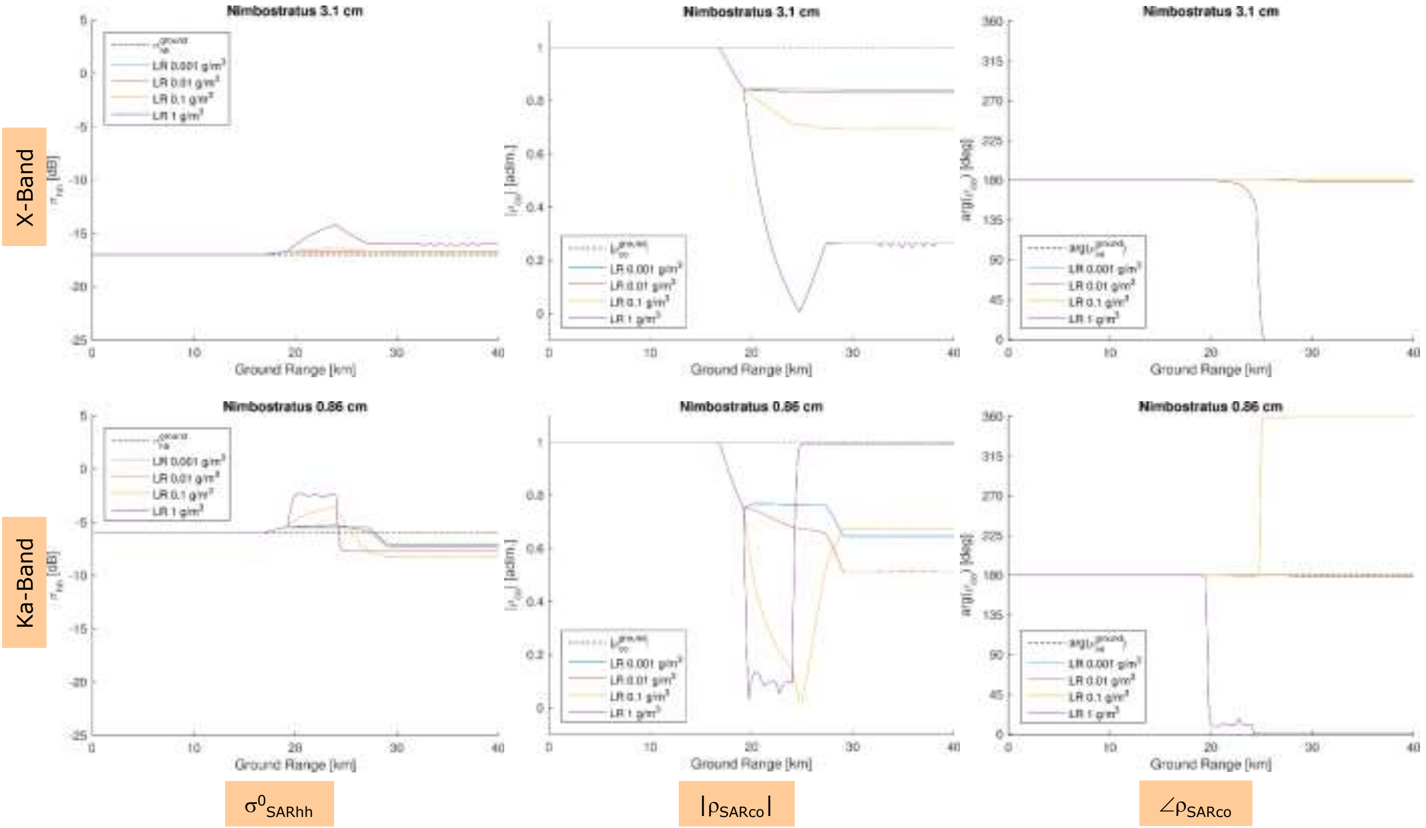

Case 2(B): Nimbostratus (frozen particles sensitivity)

- Precipitating cloud
- Ice crystals **{0.001, 0.01, 0.1, 1.0} g/m³** 2km height
- Light Raindrops **0.2 g/m³** 4km height
- Ground: dihedral corner reflectors 0.025 m

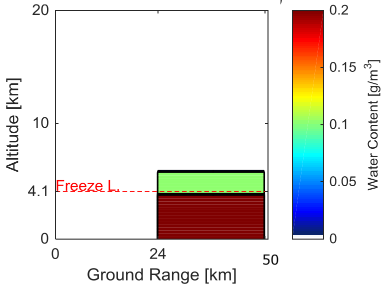

- Loss of polarimetric coherence at every band and density (at Ka only for volume component)
- Phase rotation for highest density only (@Ka > 0.01 g/m³)
- Precipitation signature at Ka for every density, at X for W >= 0.1 g/m³

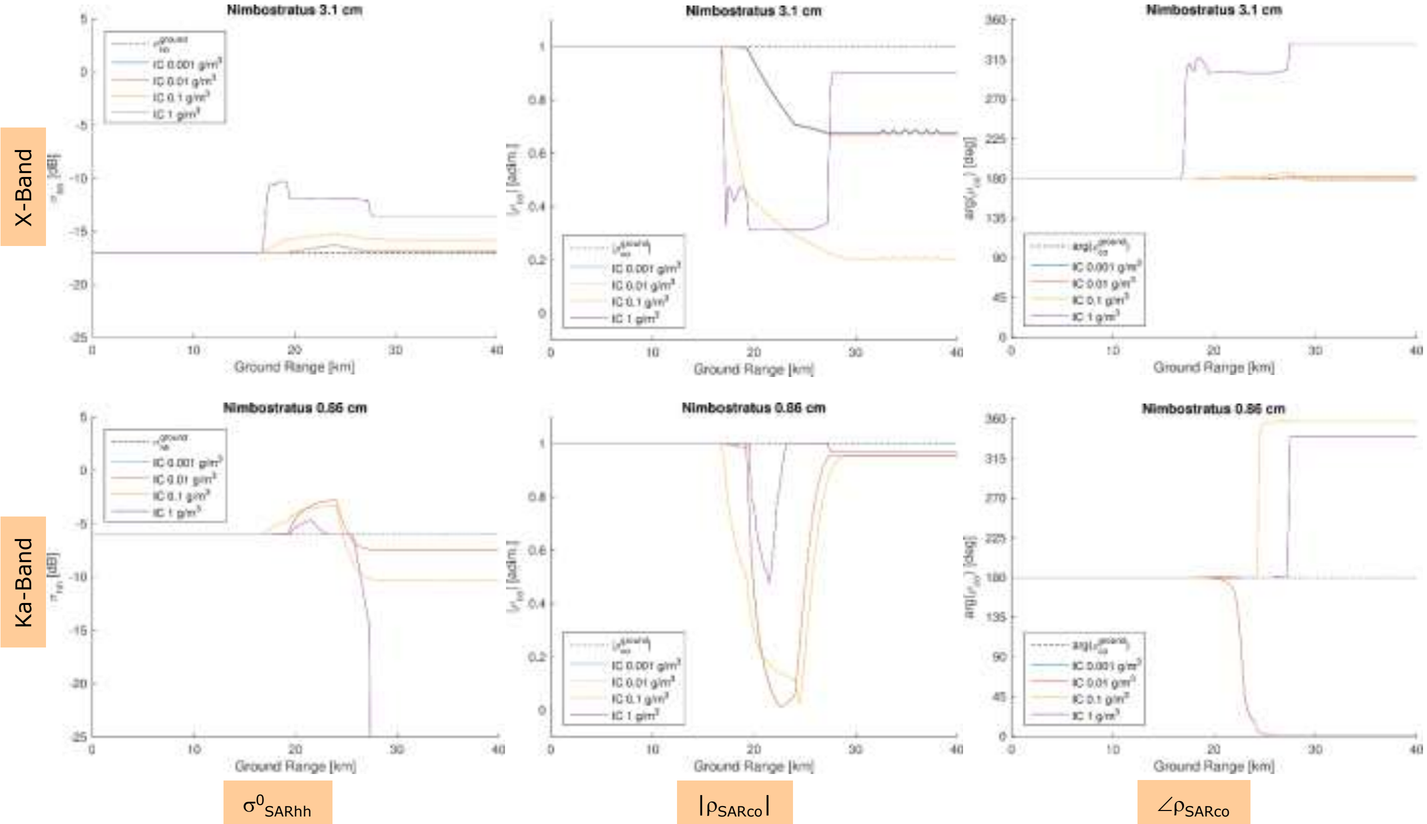

Conclusions

- **A 2D/3D simulator of the polarimetric response of a SAR in presence of precipitating clouds has been developed**
- **Considering simple synthetic clouds as well as realistic clouds predicted by a mesoscale model we found that:**
  - The impact of clouds on X and Ka band SAR can be significant, even for clouds with relatively high occurrence
  - The polarimetric signature of the ground target can be significantly modified or even completely masked
  - X Band NRCS shows an appreciable sensitivity to only "intense" events
  - Ka band confirms a great sensitivity to frozen particle, but also X band is affected
  - Complex correlation coefficient exhibits a good correlation with columnar contents.
  - SAR remote sensing of clouds has spatial resolution useful for water budget, water management and hydrological model initialization

Thank you!

Acknowledgments

This work has been partially funded by:

- European Union project Earth2Observe "Global Earth Observation for Integrated Water Resource Assessment" (http://www.earth2observe.eu)

Weinman and Marzano, JAMC, 2008
Marzano and Weinman, TGRS, 2008
Marzano et al., TGRS, 2010
Marzano et al., HESS, 2011
Marzano et al., TGRS, 2012
Pulvirenti et al., TGRS 2014
Mori et al., PolInSAR 2015
Mori et al., EOWCS 2015
Mori et al., ESA LPS 2016
Mori et al., SPIE RS 2016